



Investigation of gamma irradiation effects on the properties of CdS/p-Si heterostructure



Syed Mansoor Ali^{a,*}, Shahid Mehmood Ramay^{a,*}, Naeem Ur Rehman^b, Turki S. ALKhuraiji^c, Muhammad Ali Shar^d, Asif Mahmood^{d,e}, Ather Hassan^f, Muhammad Riaz^f

^a Department of Physics and Astronomy, College of Science, King Saud University, P.O BOX 2455, Riyadh 11451 Saudi Arabia

^b Department of Physics, Khawaja Fareed University of Engineering and Information Technology, Rahim Yar Khan, Pakistan

^c National Center for Irradiation Technology, King Abdulaziz City for Science & Technology, Saudi Arabia

^d King Abdullah Institute for Nanotechnology, King Saud University, P.O.Box, 2454, Riyadh 11451, Saudi Arabia

^e Chemical Engineering Department, College of Engineering, King Saud University, Riyadh, Saudi Arabia

^f Department of Physics, Allama Iqbal Open University, Islamabad, Pakistan

ARTICLE INFO

Keywords:

Heterostructure
Gamma irradiation
Thermal evaporation
Diffuse reflectance
Photoluminescence

ABSTRACT

Cadmium sulfide (CdS) thin films were deposited on p-type Si substrate by thermal evaporation to fabricate the CdS/p-Si heterojunction. Gamma irradiation has been used to modify the microstructural, optical and electrical characteristics of CdS/p-Si heterojunction of various doses in the range (0–80 kGy). X-ray diffraction measurements of the gamma irradiated show the reduction in crystallinity of the CdS thin films. While scanning electron microscope images depicted the average CdS particle size was found to be increased with increasing the gamma irradiation dose. Photoluminescence results revealed that at the specific dose of gamma irradiation was found to create the yellow emission in interstitial sites to the valence band. The I–V characteristics showed the current transport properties effected by the different gamma doses. The values of barrier height, saturation current and ideality factor for the CdS/p-Si heterostructure varied due to the causes like inhomogeneities in the interfacial, defect density, charge distribution on interfacial and interfacial layer thickness after gamma irradiation. The gamma irradiation induced effects and the possible mechanism in CdS/p-Si heterojunction is discussed.

1. Introduction

Cadmium sulfide (CdS) is a II–VI semiconductor and a fascinating material due to its versatile properties such as low work function, direct bandgap, excellent chemical and thermal stability, highly refractive index, good transport properties, piezoelectricity and electronic mobility [1–5]. Such properties make the CdS one of the most prominent materials in electronic and optoelectronic applications like light-emitting diodes (LEDs), nonlinear optical devices, transistors, photovoltaic cell, waveguides, photodetectors, photoelectrochemical sensors and nanogenerators [6–9]. The properties of II–VI compounds semiconductor are significantly affected by adding impurities and induced defects, that can be tuned by numerous methods such as gamma irradiation [10–13].

Several techniques have been used for CdS thin films deposition, including chemical bath deposition (CBD) [14,15], spray pyrolysis [16,17], successive ionic layer adsorption and reaction (SILAR) [18], sol-gel [19], and pulsed laser deposition (PLD) [20–22] with different

properties. The non-vacuum techniques for CdS thin film are characteristically more susceptible to corrosion and oxidation, vacuum based deposition are more appropriate for deposition of CdS thin film [23]. In vacuum based techniques the thermal evaporation is more suitable for deposition CdS thin films pinhole free, uniform and smooth thin films with required thicknesses [24].

The influences of gamma irradiation are an important concern which needs a brief description in CdS/p-Si heterostructure based devices. However, due to the high penetration power, the gamma irradiation is an effective tool for altering the structural, optical and electrical properties of materials [25–28]. It can produce the temporary and permanent effects in the heterojunction properties depends on the dose of the irradiation [29,30]. Gamma irradiation generates modification in the structure as well as in the optical and charge carriers' properties of semiconducting material. This change depends on the doses and responses of the thin films to precise irradiation [31]. However, there is just a few research on the microstructural, optical and electrical properties of heterojunction with gamma irradiation. Such as S. Pradeepa et al.

* Corresponding authors.

E-mail addresses: Symali@ksu.edu.sa (S.M. Ali), Schaudhry@ksu.edu.sa (S.M. Ramay).

investigated the effects of gamma-irradiation on the AlInGaN/AlN/GaN heterostructures with doses of 75 kGy and 150 kGy. The compositional fluctuation and intermixing of the epilayers was realized after gamma irradiation [32]. N. Shiwakoti et al. reported the modification of interface state charge transport properties of Au/n-GaP junction using the C-V and I-V measurement after gamma irradiation [33]. Ayman A. El-Amin et al. studied the (α, β, γ) irradiation effects on electrical and optical Properties of CdS / P-Si heterojunction Solar Cell [34]. M.M. El-Nahass et al. investigated the influence of gamma irradiation effects on the structural and optical properties of nanostructured InSe thin films deposited by thermally evaporation [35]. The effect of gamma irradiation on tin oxide film with different doses on interfacial properties of Au/SnO₂/n-Si was reported by N. Tugluoglu [36]. S.- Karatas et al. published the results on the influence of 60Co gamma ray irradiation on the electrical properties of an Au/n-GaAs junction irradiated to maximum dose of 500 kGy [37].

After irradiation, the gamma radiation photons lose energy and generate high energy electrons which interact with the atoms with inducing some defects or annihilating the existing defects. Such interactions may also modify the electronic configuration, structural and optical properties which causing improvement in CdS/p-Si heterostructure performance [38].

In this work, CdS/p-Si heterostructure was fabricated by coating of CdS thin films on the p-Si substrate. The novelty of the present work is to investigate the modification of micro-structural, morphological, optical and electrical characteristics of CdS thin films by different doses of gamma, which makes change in crystallinity, morphology, optical band gap and conduction mechanisms in CdS/p-Si heterojunction.

2. Materials and methods

2.1. Deposition of CdS thin films

Thin films of CdS were deposited by thermal evaporation of CdS powder (99.999% pure, Sigma Aldrich) onto the Si Substrate with substrate temperature 200 °C at pressures of 10⁻⁵ Torr. The film thickness was controlled 300 nm using a conventional quartz crystal monitor with the deposition rate of 0.5 nm s⁻¹.

2.2. Gamma Irradiation

The CdS thin films were exposed with gamma source of ⁶⁰Co (MDS Nordion company Model SC220E) with half-life of 5.2714 years, energy 1.25 MeV and rate of dose of 7.328 kGy/h. The CdS/p-Si samples were irradiated with doses 10, 20, 40, and 80 kGy. After irradiation, the top and bottom aluminum (Al) electrodes were deposited by thermal evaporator of thicknesses of 100 nm with an active area of approximately 10⁻⁵ m².

2.3. Structural measurements

The structural parameters such as average crystallite size, micro-strain and dislocation density of CdS films were calculated using formulas by XRD results [39,40]:

$$D = \frac{0.94\lambda}{\beta \cos \theta} \quad (1)$$

$$\varepsilon = \frac{\beta \cos \theta}{4} \quad (2)$$

$$\delta = \frac{1}{D^2} \quad (3)$$

Where ' λ ' is the wavelength of x-rays ($\lambda = 1.5406 \text{ \AA}$), ' θ ' is the peak angle in radian, 'D' is the crystallite size and ' β ' in radians is the full width at half maximum (FWHM).

Lattice parameters of hexagonal CdS thin films were calculated from

the XRD peak using formula [41]:

$$\frac{1}{d^2} = \frac{4(h^2 + hk + k^2)}{a^2} + \frac{l^2}{c^2} \quad (4)$$

Where 'd' is the plane spacing, h, k and l are the plane indexes and a and c are the lattice parameters of a CdS hexagonal.

2.4. Band gap calculation

The determination of band gap value (E_g) from diffuse reflectance spectra by applying the Kubelka–Munk theory gives great advantages. The Kubelka–Munk is based on the following equation [39]:

$$F(R) = \frac{(1 - R)^2}{2R} \quad (5)$$

where R is the absolute reflectance of CdS thin films; F(R) is so-called Kubelka–Munk function proportional to the extinction coefficient. F(R) values has been changed to the absorption coefficient using following equation [39]:

$$\alpha = \frac{F(R)}{t} \quad (6)$$

Where ' α ' is the coefficient of absorption and 't' is the thin film thickness.

To calculate the energy band gap of non-radiated and gamma irradiated CdS films, Kubelka–Munk absorption function ($\alpha h\nu$) was plotted against the photon energy ($h\nu$) according to equation [39]:

$$\left(\alpha h\nu \right) = \frac{F(R)h\nu}{t} = A(h\nu - E_g)^m \quad (7)$$

where 'A' is the constant, ' E_g ' is the energy band gap, ' h ' is Planck's constant value and ' ν ' is the frequency of incident photon. The value of ' m ' depends on the kind of transition of the semiconductor ($m = 2$ for indirect allowed transition) [40]. The approximated energy band gap of non-radiated and the gamma irradiated was determined from the straight line x-intercept.

2.5. Current-voltage characteristics

The I–V properties were examined by applying [40].

$$I = I_s \left[\exp\left(\frac{q(V - IR_s)}{nkT}\right) - 1 \right] \quad (8)$$

where q is the charge, V is the biased voltage, n is the ideality factor, k is the Boltzmann constant and T is temperature, I_s is the saturation current obtained from the intercept value of the straight part of ln I–V plot at zero bias, and is given by

$$I_s = AA^* \exp\left(\frac{-q\phi_b}{kT}\right) \quad (9)$$

where Φ_b is the barrier height, A is the contact area and A^* is the Richardson constant and equals to 31.6 A/cm² K² for p-type Si [39], the value of ideality factor ' n ' is measured from the gradient of the linear portion of ln (I)–V graph and given as,

$$n = \frac{q}{kT} \left(\frac{dV}{d(\ln I)} \right) \quad (10)$$

Once ' I_s ' is measured, then the barrier height can be calculated using [41]

$$\phi_b = \frac{kT}{q} \ln\left(\frac{AA^*}{I_s}\right) \quad (11)$$

The important factor that influences the electrical properties of heterojunction is the series resistance (R_s). To calculate the value of R_s , we analyzed the forward bias I–V data using Cheung's function can be

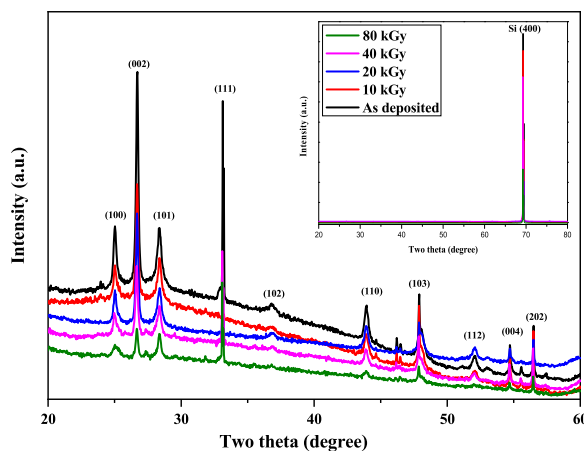


Fig. 1. The XRD results of at different gamma doses of CdS/p-Si heterostructure. (inset: for Si peak for all samples).

expressed as [42].

$$\frac{dv}{d(\ln I)} = IR_s + n \left(\frac{kT}{q} \right) \quad (12)$$

The X-ray diffraction (XRD) results of as un exposed and gamma exposed CdS thin films were collected by X-ray diffractometer (Bruker, D8 Discover) with source Cu- $\kappa\alpha$. The reflectance spectra were performed with JASCO-V 670 in range of 200–800 nm. The room temperature photoluminescence (PL) spectra of the samples were collected with excitation wavelength of 320-nm by spectrofluorometer (JESCO FP-8200). The current–voltage (I–V) characteristics were carried out by KEITHLEY 4200 SCS/CVU semiconductor characterization in dark conditions.

3. Results and discussion

The influences of gamma irradiation on the structural behaviors are characterized by X-ray diffraction (XRD). **Fig. 1** shows the XRD patterns of CdS film on Si Substrate of as deposited and irradiated with different gamma doses from 10 KGy to 80 KGy. The XRD pattern shows that all the diffraction peaks match those of the hexagonal phase structure of CdS film (JCPDS card: No. 41-1049). In addition, the Si(400) peak from the p-Si substrate is also observed (ref. JCPDS card, file no. 41-1049) as shown in the inset of **Fig. 1**. It can be seen that the intensity of the main CdS peaks decreases as the gamma dose increases, due to the induces lattice defects after radiation that can behave like a scattering centers without alteration in the crystal structure [43].

The calculated structural results by XRD are tabulate in **Table 1**. It is noticed that the crystallite size value increases due with increase the gamma dose, and the decreased micro-strain and dislocation density values. An increase in the gamma dose may cause of annihilation of structural defects that leads to decreased in density of dislocations, micro strain and an increase in the estimated average crystallites size.

Table 1
Structural parameters of the as deposited and gamma irradiated CdS/p-Si heterostructure.

Samples	Crystallite size (nm)	Micro-strain $\epsilon \times 10^{-2}$	Dislocation density $\delta \times 10^{15} \text{ m}^{-2}$	Lattice parameters	
				$a (\text{\AA})$	$c (\text{\AA})$
As deposited	73.23	12.84	0.186	4.162	6.823
10 KGy	79.54	10.32	0.158	4.158	6.796
20 KGy	89.85	8.68	0.123	4.155	6.785
40 KGy	91.41	8.28	0.119	4.154	6.737
80 KGy	93.76	7.35	0.113	4.149	6.728

Similar findings have been reported by Kozlovskiy et al. [44].

Fig. 2(a–e) shows FESEM morphology of non-radiated and gamma irradiated CdS thin films on silicon substrates at different doses. From the figure it can be seen that as deposited CdS thin film have a nanoparticle structure and the surface of the thin film is uniform and close packed with average grain size less than 78 nm. The porous structure becomes noticeable up to 40 kGy, and at 80 kGy the CdS thin films again found closed packed with large grain size of about 96 nm. The average CdS particle size was found to be increased with increase the gamma irradiation dose. It is observed morphology and crystallinity are decreased with increasing the gamma dose. As a consequence of gamma irradiation, a large amount of energy is shifted to the lattice in a short time, which is converted into the kinetic energy and may cause of thermal bursts near the surface by which the morphology and crystallinity of the irradiated thin films has decreased [45].

UV–Visible diffuse reflectance spectroscopy (UV/DRS) was used to study the optical properties of non-radiated and gamma irradiated CdS/p-Si hetrostructure with wavelength range of 200–800 nm as depicted in **Fig. 3**, it can be observed in the interference maxima and minima and the systematic wavelength shift as a result of an increase of the dose of the gamma irradiation.

The energy band gap of non-radiated and gamma irradiated CdS were obtained by Tauc's plot as shown in **Fig. 4**. The value energy band gap gets red shifted after gamma irradiation from 2.440 to 2.373 eV due to the crystallite size increase from 73.23 to 93.76 nm. This characteristic in the excitonic band is usually responsible for the properties of quantum confinement effects. The energy band gap value of the CdS thin film with increases the gamma dose resulting to decreased, as the gamma dose increases as shown in the inset of **Fig. 4**.

The energy band gap of as deposited and gamma irradiated CdS with different doses were determined, the band gap gets red shifted after gamma irradiation from 2.440 to 2.373 eV due to the crystallite size increase from 73.23 to 93.76 nm. This characteristic in the excitonic band is usually responsible for the properties of quantum confinement effects. The energy band gap value of the CdS thin film with increases the gamma dose resulting to decreased, as the gamma dose increases as shown in the inset of **Fig. 4**.

Photoluminescence (PL) is a prevailing method to examine the energy defects in the band gap, electronic structure and worth of crystalline structure of semiconductors material. The correlation between crystal structure and electronic property can be studied by photoluminescence that create from recombination of the electron traps [46]. To study the effects of different doses of gamma irradiation in formation and annihilation of energy defects and their radiative recombination, PL spectra for non-radiated and gamma irradiated CdS films at different gamma doses are presented in **Fig. 5**. It reveals that non-radiated and gamma irradiated thin films green emission (GE) centered at 512.51–512.78 nm. The cause of GE at this wavelength endorsed to the transition of donors electron from sulfur to the valence band, and conduction band to sulfur interstitial [47]. The small variation in emission peak position for the non-radiated and gamma irradiated CdS thin films due to difference in lattice parameters in crystal structure. The increase in gamma doses shifted emission peak towards longer wavelength with increase in peak intensity and with creation of a hump corresponds to yellow emission (YE). The YE is due to recombination or radiative transition from Cd atoms located in interstitial sites to the valence band [48–52]. Increase in intensity is due to enhance in sulfur vacancies after gamma irradiation and transferring towards low energy level that induced defect that increases YE and results in changing of peak position.

The energy-band diagram for CdS/p-Si heterostructure is depicted in **Fig. 6** by Anderson model. The electron affinities (4.50 and 4.05 eV) and band gap energies (2.42 and 1.12 eV) were used for CdS thin films and p-Si substrate respectively, for energy band diagram of CdS/p-Si heterostructure. The barrier energy for an electron was $\Delta E_c = \chi(\text{CdS}) - \chi(\text{Si}) = 4.50 - 4.05 = 0.45 \text{ eV}$, and the energy barrier for hole was ΔE_v

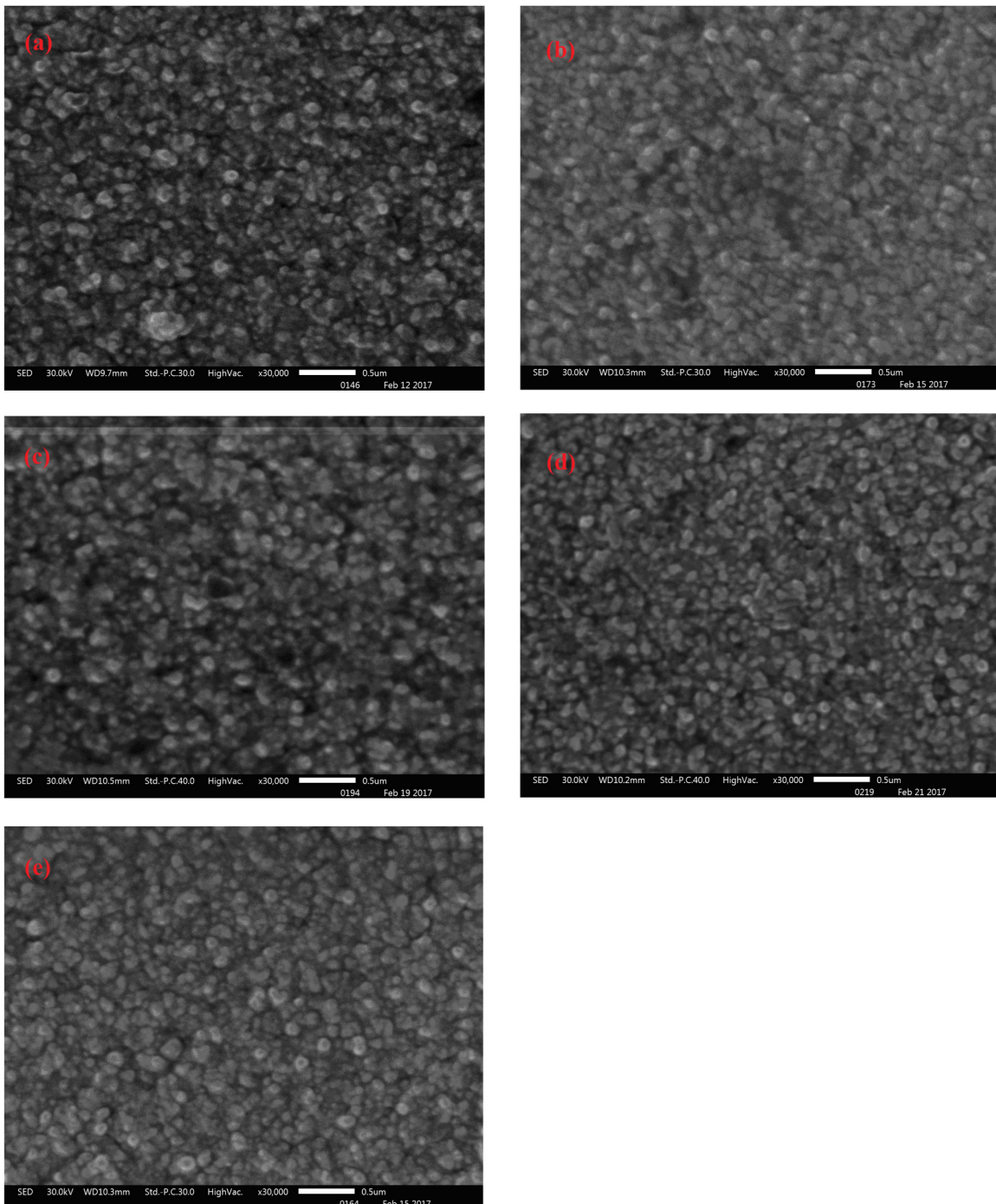


Fig. 2. SEM images of (a) as deposited, (b) 10 kGy, (c) 20 kGy, (d) 40 kGy and (e) 80 kGy CdS thin films.

$= E_g(\text{CdS}) + \Delta E_c - E_g(\text{Si}) = 2.42 + 0.45 - 1.12 = 1.75 \text{ eV}$. It is noticeable that the band break in the valence band is greater than the conduction band. So, the passage of electrons leads the forward voltage in I-V characteristic of the CdS/p-Si junction. This reveal that the CdS/p-Si junction provides a large current under forward voltage and a small current under reverse voltage.

The current-voltage (I-V) characteristics of the CdS/p-Si heterojunction at different gamma dose are shown in Fig. 7. Non-linear curves exhibit good rectification behavior. The junction parameters such diode ideality factor (n), saturation current, barrier height and series resistance (R_s) are calculated by I-V characteristics. It can be observed that the currents increase directly at low voltages (0.1–1.19 V), showing the ohmic conduction and with further increase of voltage (1.19–5.0 V),

the currents increased exponentially. It can be seen that CdS/p-Si heterojunction characteristics is a parallel shifted in both forward and reverse bias regions after the gamma irradiation and the forward and reverse current decreased with increase in the irradiation dose. The drops in the forward and reverse current values can be associated with the gamma radiation induced defects in forbidden gap. These defects are responsible for the trapping of free charge carriers and the increase of series resistance. As the gamma doses increases the density of the defects increased that caused to decrease the forward and reverse current values [53,54].

The measured values of ideality factor, saturation current and barrier heights obtained using above equations are given in Table 2. The ideality factors were measured from the $\ln(I)$ vs V graph in the biased

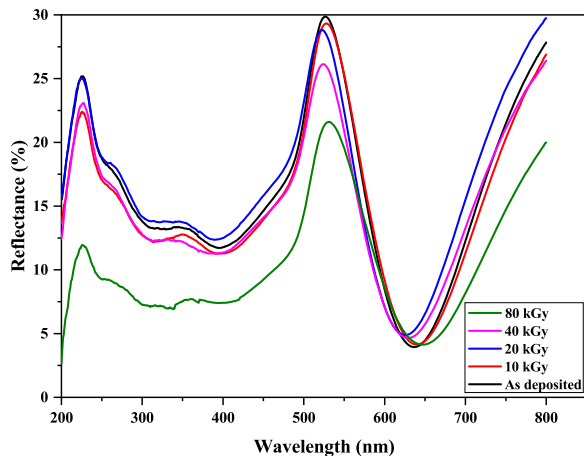


Fig. 3. Diffuse reflectance spectra at different level of gamma doses of CdS/p-Si heterostructure.

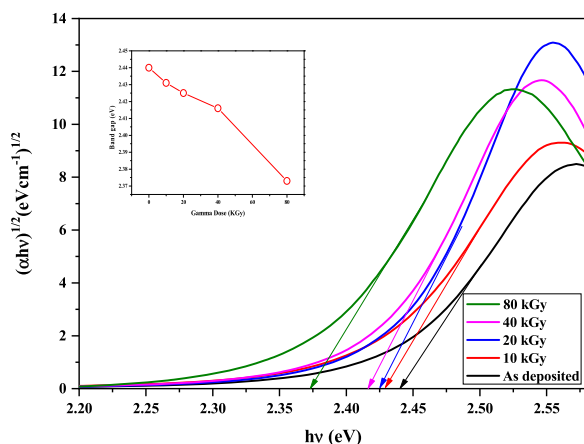


Fig. 4. Tauc's plot of non-radiated and with different gamma dose irradiated of CdS/p-Si heterostructure. (Inset: the trend of band gap energy with doses).

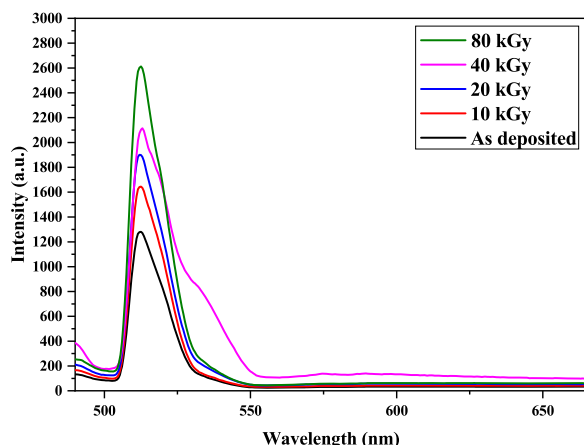


Fig. 5. PL spectra of as deposited and gamma irradiated CdS/p-Si heterostructure.

voltage from 0 to 0.4 V. The decreased in ideality factor and saturation current shows that there is a dynamic equilibrium in dual different approaches of defects creation and annealing by gamma irradiation. Similar results have also been noticed by Srour et al. [55]. The barrier height actually the potential barrier at the interface of the CdS and Si, the decrease in the forward and reverse current means the decrease charge carriers flow of in the CdS/p-Si heterojunction. That can be

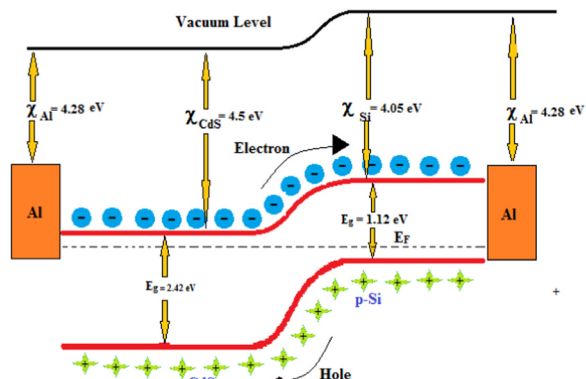


Fig. 6. Energy band diagram of CdS/p-Si heterostructure.

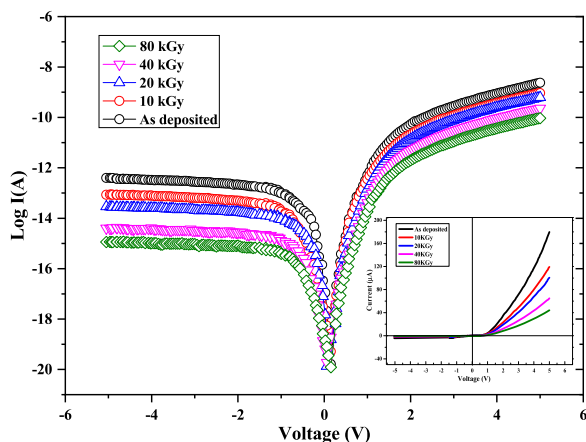


Fig. 7. LogI-V graph of non-radiated and different doses of gamma irradiated CdS/p-Si heterostructure. (Inset: I-V characterization non-radiated and different doses of gamma irradiated CdS/p-Si heterostructure).

Table 2
I-V characteristics parameters of CdS/p-Si heterojunction.

Gamma irradiation (kGy)	'n'		Saturation Current ' I_s ' (A $\times 10^{-3}$)	Barrier Height ' Φ_B ' (eV)	Series resistance ' R_s ' (kΩ)
	InI-V	Cheung's method			
Non-radiated	5.32	5.56	7.32	0.53	6.53
10	4.93	4.87	5.83	0.55	18.94
20	4.78	4.75	5.56	0.57	21.59
40	4.69	4.64	5.28	0.58	23.21
80	4.57	4.36	4.49	0.61	25.67

concluded that the increase in the barrier height with increased the gamma doses.

Fig. 8 depicts the Cheung's plot between the $dV/dln(I)$ versus I for different gamma doses. The slope and y-axis intercept of this plot give R_s and nkT/q values respectively. This can be seen from Fig. 8, the plots revealed very straight line for non-radiated and all gamma irradiated samples. When the gamma doses increased, the corresponding plot was shifted upward. The R_s value increased with increasing gamma doses. This increase is supposed to be due to the same argument before, where the increment in the gamma dose is caused more radiation-induced traps.

4. Conclusions

The effects of different doses of gamma irradiation on microstructural, optical and I-V properties CdS/p-Si has been investigated.

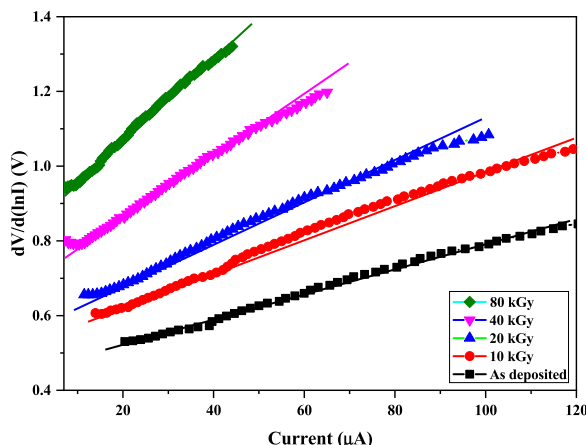


Fig. 8. Cheung Plot's of non-irradiated and different gamma dose irradiated CdS/pSi heterostructure.

The influence of gamma doses was observed. The XRD measurements show the CdS thin films was nanocrystalline and the crystallinity of the CdS thin film decreases as the gamma dose increases. SEM results reveal that at specific gamma dose the CdS thin films became closed packed with large grain size of about 96 nm. The effects of gamma irradiation noted on optical band gap that shifted from 2.440 to 2.373 eV due to the crystallite size increase from 73.23 to 93.76 nm. The PL peak transferred towards low energy level due to the induced defect which increases YE with increasing the gamma doses. In addition, the parameters such as barrier height, ideality factor and saturation current as well as current – voltage have been studied. As increasing gamma doses, the barrier height increased and the ideality factor and saturation current decreased.

Acknowledgements

The authors would like to extend his sincere appreciation to the Deanship of Scientific Research at King Saud University, Riyadh Saudi Arabia for funding under Research Group (No. RG 1435-004)

References

- [1] T.Y. Zhai, Z.J. Gu, H.Z. Zhong, Y. Dong, Y. Ma, H.B. Fu, Y.F. Li, J.N. Yao, Cryst. Growth Des. 7 (2007) 488.
- [2] M. Zhang, T.Y. Zhai, X. Wang, Q. Liao, Y. Ma, J.N. Yao, J. Solid State Chem. 182 (2009) 3183.
- [3] Y.B. Hahn, Korean J. Chem. Eng. 28 (2011) 1797.
- [4] Y.F. Lin, J. Song, Y. Ding, S.Y. Lu, Z.L. Wang, Adv. Mater. 20 (2008) 3127.
- [5] Y.F. Lin, J. Song, Y. Ding, S.Y. Lu, Z.L. Wang, Appl. Phys. Lett. 92 (2008) 22105.
- [6] N.V. Hullavarad, S.S. Hullavarad, P.C. Karulkar, J. Nanosci. Nanotechnol. 8 (2008) 3272.
- [7] S. Kar, S. Chaudhuri, Synth. React. Inorg. Met. 36 (2006) 289.
- [8] M.I.B. Utama, J. Zhang, R. Chen, X. Xu, D. Li, H. Sun, Q. Xiong, Nanoscale 4 (2012) 1422.
- [9] C. Wang, Y. E, L. Fan, Z. Wang, H. Liu, Y. Li, S. Yang, Y. Li, Adv. Mater 19 (2007), p. 3677.
- [10] S. Del Sordo, L. Abbene, E. Caroli, A.M. Mancini, A. Zappettini, P. Ubertini, Sensors 9 (2009) 3491.
- [11] M. Ashry, S.A. Fayek, Renew. Energy 23 (2001) 441.
- [12] S. Kasap, P. Capper, Springer Handbook of Electronic and Photonic Materials, Springer, 2006.
- [13] M.R. Balboul, H.M. Hosni, S.A. Fayek, 81, 2012, 1848.
- [14] A. Cortes, H. Gomez, Sol. Energy Mater. Sol. Cells 82 (2004) 21.
- [15] H. Moualkia, S. Hariech, M.S. Aida, N. Attaf, E.L. Laifa, J. Phys. D: Appl. Phys. 42 (2009) 135404.
- [16] K. Ravichandran, P. Philominthan, Appl. Surf. Sci. 255 (2009) 5736.
- [17] R.K. Sharma, K. Jain, Curr. Appl. Phys. 3 (2003) 199.
- [18] B. Ghosh, S. Chowdhury, P. Banerjee, S. Das, Thin Solid Films. 519 (2011) 3368.
- [19] H. Sakai, T. Tamaru, T. Sumomogi, H. Ezumi, B. Ullrich, Jpn. J. Appl. Phys. 37 (1998) 4149.
- [20] D.M. Bagnall, B. Ullrich, X.G. Qiu, Y. Segawa, H. Sakai, Opt. Lett. 24 (1999) 1278.
- [21] B. Ullrich, R. Schroeder, H. Sakai, A. Zhang, S.Z.D. Cheng, Appl. Phys. Lett. 80 (2002) 356.
- [22] M. Thambidurai, S. Agilan, N. Muthukumarasamy, N. Murugan, R. Balasundaraprabhu, Int. J. Nanotechnol. Appl. 3 (2009) 29.
- [23] S.G. Hur, E.T. Kim, J.H. Lee, G.H. Kim, S.G. Yoona, J. Vac. Sci. Technol. B. 26 (2008) 1334.
- [24] N. Memariani, S.M. Rozati, I. Concina, A. Vomiero, Materials 10 (2017) 773.
- [25] D.C. Sheridan, G. Chung, S. Clark, J.D. Cressler, IEEE Trans. Nucl. Sci. 48 (2012) 2229.
- [26] G.A. Umana-Membreno, J.M. Dell, G. Parish, B.D. Nener, L. Faraone, U.K. Mishra, IEEE Trans. Electron Dev. 50 (2003) 2326.
- [27] H. Uslu, M. Yıldırım, S. Altindal, P. Durmus, Radiat. Phys. Chem. 81 (2012) 362.
- [28] Ö. Gülli, M. Çankaya, M. Biber, A. Türüt, J. Phys. D: Appl. Phys. 41 (2008) 135103.
- [29] N. Tuğluoğlu, S. Karadeniz, Ö.F. Yüksel, et al., Indian J. Phys. 89 (2015) 803.
- [30] Y.S. Ocak, T. Kılıçoglu, G. Topal, M.H. Baskan, Nucl. Instrum. Methods A 612 (2010) 360.
- [31] A.G. Holmes-Siedle, L. Adams, Handbook of Radiation Effects, Oxford University Press, Oxford, New York, 1993.
- [32] S. Pradeepa, R. Loganathan, S. Surendera, K. Prabakarana, K. Asokan, K. Baskar, Super. Lattices Microstruct. 120 (2018) 40.
- [33] N. Shiwakoti, A. Bobby, K. Asokan, B. Antony, Mater. Sci. Semicond. Process. 74 (2018) 1.
- [34] A.A. El-Amin, M.H. Saad, J. Mater. Sci. Res. 7 (2018) 20.
- [35] A. Bobby, N. Shiwakoti, S. Verma, P.S. Gupta, B.K. Antony, Mater. Sci. Semicond. Process. 21 (2014) 116.
- [36] M.M. El-Nahass, A.A.A. Darwish, E.F.M. El-Zaidia, A.E. Bekheet, J. Non-Cryst. Solids 382 (2013) 74–78.
- [37] N. Tugluoglu, Nucl. Instrum. Methods Phys. Res. B 254 (2007) 118.
- [38] S. Karatas, A. Turut, S. Altindal, Nucl. Instrum. Methods Phys. Res. B 555 (2005) 260.
- [39] S.M. Ali, J. Mater. Sci: Mater. Electron 28 (2017) 16314.
- [40] K. Ejderha, N. Yıldırım, A. Turat, Superlattice Microstruct. 47 (2010) 241.
- [41] S.M. Sze, Physics of Semiconductor Devices, Wiley Eastern, New York, 1993.
- [42] S.K. Cheung, N.W. Cheung, Appl. Phys. Lett. 49 (1986) 85.
- [43] H.H. Mahmoud, I.K. Battisha, F.M. Ezz-Eldin, Spectrochim. Acta Part A: Mol. Biomol. Spectrosc. 150 (2015) 72.
- [44] A. Kozlovskiy, K. Dukenbayev, I. Ivanov, S. Kozin, V. Aleksandrenko, A. Kurakhmedov, E. Sambaev, I. Kenzhina, D. Tosi, V. Loginov, M. Zdrovovets, Mater. Res. Express 5 (2018) 65502.
- [45] K. Abhirami, P. Matheswaran, B. Gokul, R. Sathyamoorthy, D. Kanjilal, K. Asokan, Vacuum 90 (2013) 39.
- [46] S. Ravishankar, A.R. Balu, M. Anbarasi, V.S. Nagarethnam, Optik 126 (2015) 2550.
- [47] N. Manjula, K. Usharani, A.R. Balu, V.S. Nagarethnam, Int. J. ChemTech Res. 6 (2014) 705.
- [48] O. Vigil, I. Riech, M.R. Garcia, O.J.A. Zelaya, Vac. Sci. Tech. A. 15 (1997) 2282.
- [49] M.R. Lozada, A.O. Zelaya, Thin Solid Films 386 (1996) 281.
- [50] P. Kumar, N. Saxena, R. Chandra, V. Gupta, A. Agarwal, D. Kanjilal, Nanoscale Res. Lett. 7 (2012) 584.
- [51] P. Kumar, N. Saxena, R. Chandra, K. Gao, S. Zhou, A. Agarwal, F. Singh, V. Gupta, D. Kanjilal, J. Lumin. (2014) 147.
- [52] S. Chandramohan, R. Sathyamoorthy, P. Sudhagar, D. Kanjilal, D. Kabiraj, K. Asokan, V. Ganesan, T. Shripathi, U.P. Deshpande, Appl. Phys. A: Mater. Sci. Process. 94 (2009) 703.
- [53] K. Çınar, C. Coşkun, Ş. Aydoğan, H. Asıl, E. Gür, Nucl. Instrum. Methods Phys. Res. B 268 (2010) 616.
- [54] Z. Lin, Z. Yi-Men, Z. Yu-Ming, H. Chao, J. Semicond. 31 (2010) 114006.
- [55] J.R. Srour, C.J. Marshall, P.W. Marshall, Review of displacement damage effects in silicon devices, IEEE Trans. Nucl. Sci. 50 (2003) 653.